CALCULATED TRAVEL TIMES OF SEISMIC CORE WAVES*

By R. D. Forester

ABSTRACT

Travel times for the seismic core waves, PKP, PKS, and SKS, were computed by integration along the travel paths. For this purpose the velocity distribution within the earth was broken into segments which were represented by continuous functions. Except for rays of grazing incidence to the outer core the times calculated for PKP and PKS are intermediate between the smoothed times given by Jeffreys and times based upon recent observed data. The times calculated for SKS are in fair agreement with the smoothed times given by Jeffreys.

Introduction

In order to estimate the intensity of energy flux expected for seismic waves at various epicentral distances along the earth's surface, travel times must be known with a high degree of precision. This is especially true near a focal point, where the slope of the travel-time curve changes rapidly. Observed travel-time data are frequently not precise enough for a determination of the curvature of the travel-time

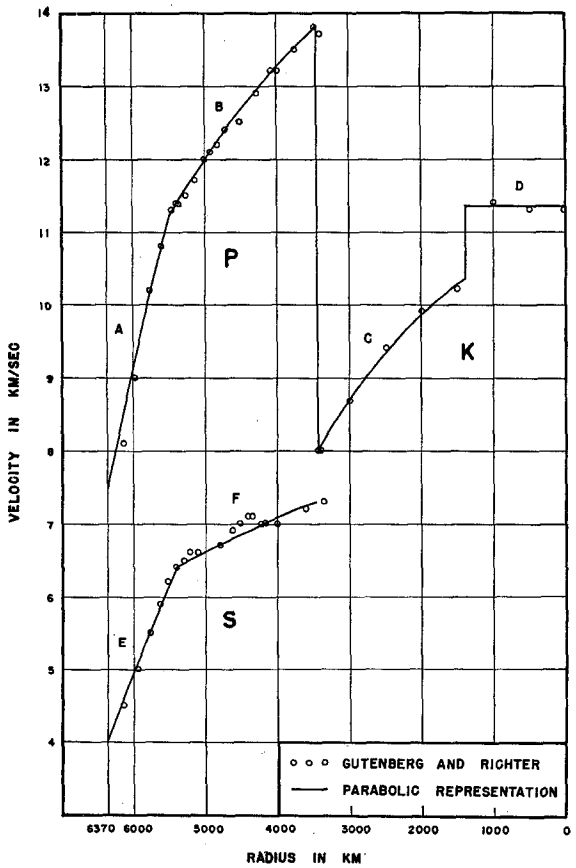

Fig. 1.

* Manuscript received for publication August 3, 1954.

curves, a factor which is crucial in the analysis of the energy content of seismic waves. It was this fact which prompted the writer in his study of the energy content of the seismic core wave PKS to devise a method for computing its travel times. Travel times for PKP and SKS were computed as an additional check on the effectiveness of the computational method.

Computational Method

The travel times were computed directly by integration along the travel paths. Use was made of velocities for the mantle and the core given by Gutenberg and Richter. (See fig. 1.) These velocities are listed, respectively, in tables 69 and 73 of Gutenberg (1951*b*). The large magnitude of the gradients of these velocities indicates that large errors would result if constant velocities, and hence straight ray paths, were assumed for transverse waves in the mantle, and for longitudinal waves in the mantle and in the core. Instead, the velocity curves were broken into six segments, designated by the letters A through F. Segments A and B (longitudinal velocities in the core) and segments E and F (transverse velocities in the mantle) were expressed by the parabolic function: (1)

TABLE 1

Boundary Conditions for the Calculation of the Travel-Time Curves

Segment	r_1	r_2	v_1	v_2
	km × 10^{-3}	km × 10^{-3}	km/sec.	km/sec.
A, B — P	5.50	6.37	11.2	7.5
	3.45	5.50	13.8	11.2
C, D — K	1.37	3.45	10.35	8.0
	0.00	1.37	11.35	11.35
E, F — S	5.40	6.37	6.40	4.00
	3.45	5.40	7.30	6.40

$$V = V_0 - Kr^2$$

where r is the radius from the center of the earth, and V_0 and K are constants. The ray paths corresponding to such a velocity function are arcs of circles.

Since the velocity discontinuity at the inner core boundary appears to be gradational, continuous travel times were computed for only those waves which travel through the outer core. The segment D (velocity of the inner core) was assumed to be constant, and was used to calculate the travel times of only those waves which travel diametrally through the earth. Segments A, B, and C were used to compute the travel times of PKP; segments E, F, and C, those of SKS; and segments A, B, C, E, and F, those of PKS.

The boundary conditions imposed on equation 1 in order to evaluate the parameters V_0 and K are shown in table 1. As shown in figure 1, the agreement between the parabolic representation of the velocities and the data of Gutenberg and Richter is close.

If the boundary conditions in table 1 are substituted into equation (1), two simultaneous linear equations result which can be solved for V_0 and K:

$$V_0 = \frac{v_1 r_2^2 - v_2 r_1^2}{r_2^2 - r_1^2} \tag{2}$$

$$K = \frac{v_1 - v_2}{r_2^2 - r_1^2} \tag{3}$$

Where r_1 = inner radius bounding a ray-path segment
r_2 = outer radius bounding a ray-path segment
v_1 = velocity where inner radius bounds a ray-path segment
v_2 = velocity where outer radius bounds a ray-path segment.

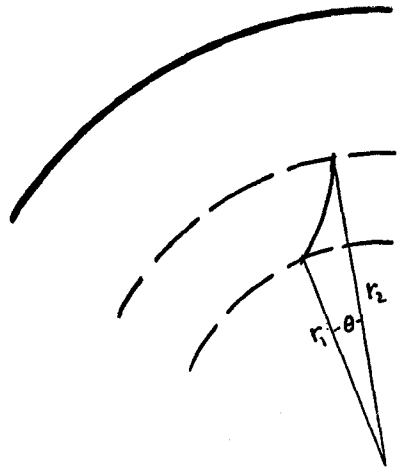

Fig. 2.

By the application of Fermat's principle of stationary time, it can be shown that the central angle subtended by a ray-path segment for the velocity function defined by equation (1) is:

$$\theta = \tfrac{1}{2}\left\{ \arcsin\left[\frac{1 + 2p^2V_0K - 2p^2K^2r_2^2}{\sqrt{1 + 4p^2V_0K}}\right] + \arcsin\left[\frac{1 + 2p^2V_0K - \frac{2p^2V_0^2}{r_2^2}}{\sqrt{1 + 4p^2V_0K}}\right] \right.$$
$$\left. - \arcsin\left[\frac{1 + 2p^2V_0K - 2p^2K^2r_1^2}{\sqrt{1 + 4p^2V_0K}}\right] - \arcsin\left[\frac{1 + 2p^2V_0K - \frac{2p^2V_0^2}{r_1^2}}{\sqrt{1 + 4p^2V_0K}}\right] \right\} \tag{4}$$

where "p" is equal to the ray parameter. Similarly, it can be shown that the corresponding time of travel along a ray path segment is:

$$t = \frac{1}{2\sqrt{V_0K}} \log_{10} \left| \frac{1 - \frac{v_2}{2V_0} + \sqrt{1 - \frac{v_2}{V_0} - p^2\frac{v_2^2}{V_0}K}}{1 - \frac{v_1}{2V_0} + \sqrt{1 - \frac{v_1}{V_0} - p^2\frac{v_1^2}{V_0}K}} \times \frac{v_1}{v_2} \right| \tag{5}$$

Values for V_0 and K can be evaluated from equations (2) and (3), respectively. If the ray path does not penetrate as deep as the inner boundary radius, r_1, the expression for the central angle reduces to:

TABLE 2

CALCULATED TRAVEL TIMES

$1/V$	Δ PKP	t PKP	Δ PKS	t PKS	Δ SKS	t SKS
sec/deg.	deg.	sec.	deg.	sec.	deg.	sec.
0.000	180.000	1201.06	180.000	1416.09	180.000	1631.13
2.310	149.345	1186.60	142.776	1393.77	136.207	1600.94
2.319	149.264	1186.41	142.663	1393.50	136.061	1600.58
2.383	148.688	1185.06	141.838	1391.56	134.988	1598.06
2.446	148.136	1183.73	141.031	1389.61	133.926	1595.50
2.510	147.610	1182.42	140.241	1387.66	132.873	1592.89
2.574	147.109	1181.14	139.470	1385.69	131.831	1590.24
2.638	146.637	1179.92	138.719	1383.74	130.801	1587.55
2.701	146.193	1178.74	137.987	1381.78	129.780	1584.83
2.765	145.781	1177.60	137.276	1379.83	128.771	1582.07
2.828	145.400	1176.54	136.586	1377.91	127.772	1579.28
2.892	145.052	1175.55	135.918	1376.00	126.784	1576.45
2.955	144.740	1174.63	135.274	1374.11	125.808	1573.60
3.018	144.466	1173.82	134.654	1372.27	124.841	1570.72
3.082	144.231	1173.10	134.059	1370.45	123.886	1567.80
3.145	144.040	1172.50	133.491	1368.68	122.942	1564.86
3.208	143.894	1172.05	132.951	1366.97	122.009	1561.90
3.271	143.797	1171.72	132.442	1365.31	121.087	1558.90
3.334	143.757	1171.58	131.966	1363.74	120.176	1555.90
3.397	143.765	1171.63	131.520	1362.25	119.275	1552.87
3.460	143.841	1171.89	131.113	1360.85	118.385	1549.82
3.523	143.985	1172.38	130.746	1359.56	117.507	1546.74
3.586	144.205	1173.17	130.422	1358.41	116.638	1543.66
3.649	144.510	1174.28	130.146	1357.42	115.781	1540.56
3.711	144.913	1175.76	129.924	1356.59	114.934	1537.42
3.774	145.426	1177.68	129.762	1356.00	114.098	1534.31
3.836	146.067	1180.10	129.669	1355.62	113.272	1531.15
3.899	146.859	1183.18	129.658	1355.60	112.457	1528.01
3.961	147.834	1187.02	129.743	1355.93	111.651	1524.85
4.023	149.037	1191.82	129.947	1356.75	110.856	1521.68
4.086	150.535	1197.89	130.303	1358.20	110.071	1518.50
4.148	152.434	1205.72	130.866	1360.52	109.298	1515.31
4.210	154.932	1216.16	131.734	1364.14	108.536	1512.11
4.272	158.459	1231.12	133.119	1370.00	107.780	1508.91
4.334	164.504	1257.29	135.769	1381.49	107.034	1505.69
4.363	174.199	1299.38	140.442	1401.79	106.686	1504.20

$$\theta = \tfrac{1}{2}\left\{\arcsin\left[\frac{1 + 2p^2V_0K - 2p^2Kr_2^2}{\sqrt{1 + 4p^2V_0K}}\right] + \arcsin\left|\frac{1 + 2p^2V_0K - \frac{2p^2V_0^2}{r_2^2}}{\sqrt{1 + 4p^2V_0K}}\right|\right\} \tag{6}$$

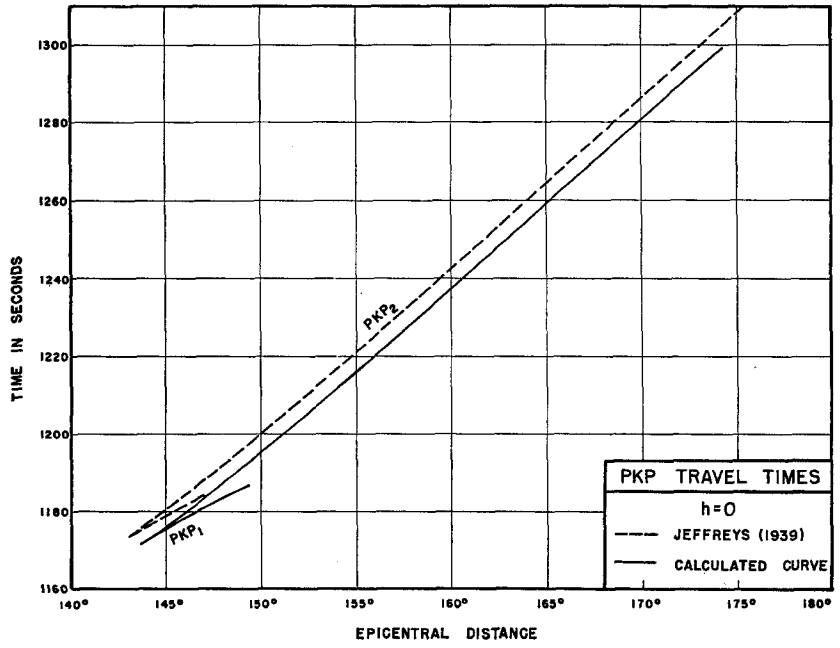

Fig. 3.

whereas the expression for the time becomes more complicated:

$$t = \frac{1}{2\sqrt{V_0K}} \log_{10}\left|\frac{2\frac{V_0}{v_2} - 1 + 2\sqrt{\frac{V_0^2}{v_2^2} - p^2V_0K - \frac{V_0}{v_2}}}{\frac{4p^2V_0K}{\sqrt{1 + 4p^2V_0K} - 1} - 1}\right| \tag{7}$$

The travel times and the central angles of the component segments of the core phases were computed from equations (4), (5), (6), and (7). These travel times and central angles were then combined, respectively, to obtain the total travel time as a function of the epicentral distance. In table 2, the resultant travel times for the core phases are listed as a function of the ray parameter. The ray parameter is equal to the reciprocal of the apparent velocity of a wave front as it emerges at the earth's surface, and hence is equal to the slope of the travel-time curve, $dt/d\Delta$, at the corresponding epicentral distance.

Results

In figures 3, 4, and 5, the calculated travel times can be compared with the smoothed travel times given by Jeffreys (1939*b*). The calculated times for PKP are several

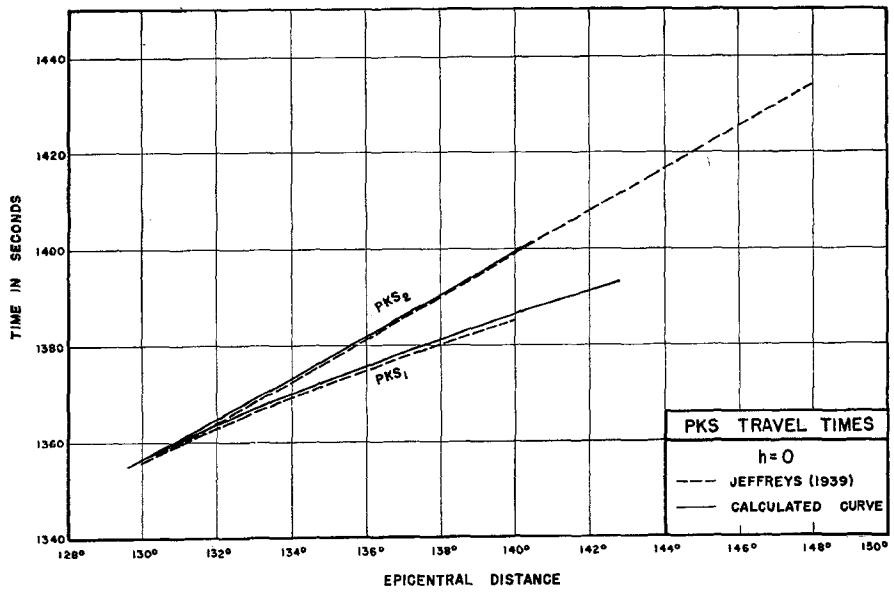

Fig. 4.

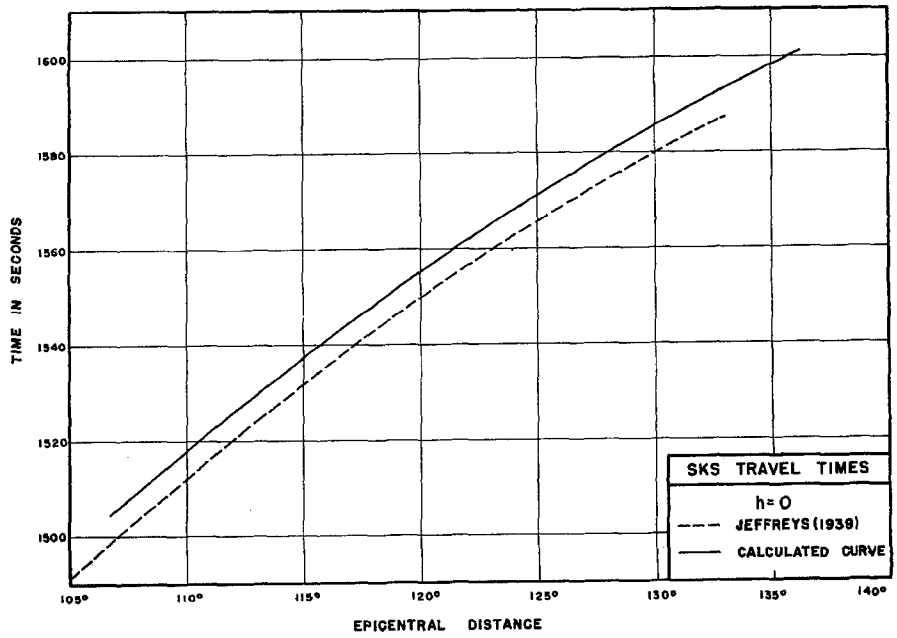

Fig. 5.

seconds later than the smoothed times of Jeffreys; those for PKS, about equal to those of Jeffreys; and those for SKS, several seconds earlier than those of Jeffreys. Actually, the calculated times for PKP, PKS, and SKS would all be expected to be a few seconds earlier than the smoothed times of Jeffreys because the calculated

times were computed from velocity functions for the mantle which did not incorporate the low velocities which prevail in the crust.

The paths computed for rays which graze the core are highly sensitive to the velocity assumed to exist outside the core boundary. The function used to represent the longitudinal velocity near the core did not follow the sharp decrease in velocity

TABLE 3

TRAVEL-TIME COMPARISONS OF CORE PHASES

Phase	Smoothed travel times of Jeffreys (1939)		Calculated travel times	
	Epicentral distance	Time	Epicentral distance	Time
	deg.	sec.	deg.	sec.
PKP through center of earth	180	1212.2	180	1201.1
PKS through center of earth	180	1422.9	180	1416.1
SKS through center of earth	180	1633.5	180	1631.1
PKP focus	143	1173.5	143.8	1171.6
PKS focus	130	1356.2	129.6	1355.6
PKP grazing outer core	180	1330.6	174.2	1299.4
PKS grazing outer core	148	1435.0	140.4	1401.8
SKS maximum angle of incidence to outer core	62	1213.7	63.7	1232.3
PKP grazing inner core	147	1184.1	149.3	1186.6
PKS grazing inner core	140	1385.7	142.8	1393.8
SKS grazing inner core	133	1587.3	136.2	1600.9

gradient near the core boundary indicated by Gutenberg and Richter. (See fig. 1.) This may account for the fact that the distances computed for the PKP and PKS rays which graze the outer core were too small.

Listed in table 3 are some key comparisons between the calculated times and the smoothed times of Jeffreys. The focal point data for PKP and PKS are in excellent agreement. The largest discrepancies occur for the waves which graze the outer core.

The epicentral distance of the PKP_2 ray which grazes the outer core was computed as 174°.2. Jeffreys gives a figure of 180° for this distance. Jeffreys' figure is more valid because Gutenberg and Richter (1934) have observed PKP_2 at a maximum distance of 180°.

The distance of the PKS_2 ray which grazes the outer core was computed as 140°.4. Jeffreys gives a figure of 148° for this distance. Neither figure compares favorably with a distance of 143° predicted from a travel-time curve (hereafter designated as the "synthetic" PKS travel-time curve) synthesized by the method of Wadati and Masuda (1934) from travel times given by Jeffreys (1939*a*) for PcS and from travel times given by Gutenberg (1951*a*) for K.

For PKP and SKS, the slopes of the calculated curves match those of Jeffreys rather well; for PKS, they diverge noticeably. For the rays which penetrate close to the inner core, the slopes of the calculated curves would be expected to be significantly larger than those of the curves of Jeffreys, because Jeffreys (1952) calculates higher velocities for longitudinal waves in the outer core than does Gutenberg (1951*a*). (See fig. 6.)

For PKP, the calculated curve agrees better with the observed data of Denson (1952) than does the curve of Jeffreys. The focal point for the calculated curve occurs at 143°.8, and that for the curve of Jeffreys at 143°. Denson, from a consideration of amplitude data, concludes that the focal distance for long-period waves occurs at 143°, and that for short-period waves at 147°. The distance of the PKP_1

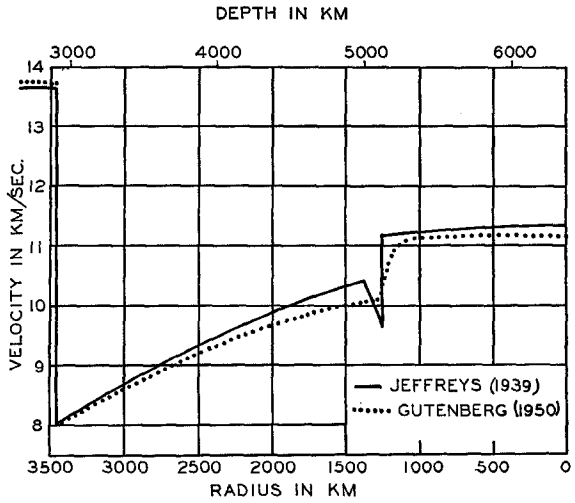

Fig. 6. Calculated velocity of longitudinal waves in the core.

ray which grazes the inner core is 149°.3 for the calculated curve, and 147° for the curve of Jeffreys. Denson believes this distance to be about 157°.

For PKS, the main focal branch of the calculated curve, PKS_1, agrees somewhat better with the observed data than does the curve of Jeffreys. The focal point of PKS occurs at 129°.6 for the calculated curve and at 130° for the curve of Jeffreys. Forester (1953) has observed that the focal point occurs at 131½° for waves with periods of 1 to 5 seconds, and between 130 and 131° for waves with periods of 5 to 10 seconds.

The epicentral distance of the PKS_1 ray which grazes the inner core is 142°.8 for the calculated curve, 140° for the curve of Jeffreys, and 149° for the synthetic PKS curve. Long-period PKS waves have been observed with certainty by Forester (1953) at a maximum distance of 145°.

The epicentral distances at which the PKP_1 and PKS_1 rays graze the inner core is less for the calculated curves than for the curves of Jeffreys, partly because Jeffreys has calculated 130 km. less depth to the inner core than has Gutenberg; and partly because Jeffreys has calculated core velocities which have higher gradients than has Gutenberg. (See fig. 6.) High-velocity gradients produce greater ray curvature, and accordingly cause the central angle subtended by a ray in the core to be reduced.

The slopes of PKS_1 for the calculated curve are higher than those for the curve of Jeffreys and lower than those for the synthetic PKS curve. The slopes of PKS_2 are lower for the calculated curve than those for either the curve of Jeffreys or the synthetic curve. Forester has observed slopes for PKS_1 more in accord with the calculated curve than the curve of Jeffreys.

Conclusions

Travel times which are calculated by approximating the velocity distribution within the earth by an assemblage of continuous functions provide a basis for the unification and comparison of different types of seismic waves with each other. Such travel times can be calculated with a precision not attainable from observed data, and hence may be used as smoothed travel times where the observed data are crude, or as predicted travel times where observed data are lacking.

Travel times for rays which graze a discontinuity are difficult to calculate, for such rays are highly sensitive to the velocity proximal to the discontinuity.

Calculated travel times should aid in the attempt to correlate multiples of different seismic phases with each other, to analyze dispersion, and to detect where seismic ray paths might deviate markedly from the ray paths defined by Fermat's principle of stationary time.

To be of value, calculated travel times must be not only precise, but accurate. They are not a substitute for observed data. Wherever possible, they should be systematically adjusted to agree with the observed data.

References

Denson, M. E., Jr.
1952. "Longitudinal Waves through the Earth's Core," *Bull. Seism. Soc. Am.*, 42: 119–134.

Forester, R. D.
1953. "Studies of the Travel Times, Periods, and Energy of Seismic Waves SKP and Related Phases," unpublished doctoral dissertation, California Institute of Technology, Pasadena, California.

Gutenberg, B.
1951*a*. "PKKP, P'P', and the Earth's Core," *Trans. Am. Geophys. Union*, 32: 373–390.
1951*b*. *Internal Constitution of the Earth* (Dover Pub.).

Gutenberg, B., and C. F. Richter
1934. "On Seismic Waves (First Paper)," *Gerlands Beitr. z. Geophysik*, Vol. 5, pp. 56–133.

Jeffreys, H.
1939*a*. "The Time of PcP and ScS," *Mon. Not. Roy. Astron. Soc., Geophys. Suppl.*, 4: 337–547.
1939*b*. "The Times of Core Waves (Second Paper)," *ibid.*, 4: 594–615.
1952. *The Earth* (Cambridge Univ. Press), p. 115.

Wadati, K., and K. Masuda
1934. "On the Travel Time of Earthquake Waves, Part VI," *Geophys. Mag.*, Tokyo, 8: 187–194.

California Institute of Technology
Pasadena, California
(Division of the Geological Sciences, contribution no. 689)